Micromechanics-based durability study of cellulose cement in flexure

P.J. Kim [a,*], H.C. Wu [a], Z. Lin [a], V.C. Li [a], B. deLhoneux [b], S.A.S. Akers [c]

[a]*Advanced Civil Engineering Materials Research Laboratory, Department of Civil and Environmental Engineering, University of Michigan, Ann Arbor, Michigan 48109, USA*
[b]*Redco N.V., R&D Center, Kapelle-Op-den-Bos, Belgium*
[c]*Eternit AG, R&D Center, Niederurnen, Switzerland*

Abstract

A micromechanics-based durability model was developed to predict the flexural mechanical properties of thin sheet cementitious composites reinforced with refined and unrefined cellulose fibers when the composite was tested dry, wet, and accelerated (carbonation) aged. The model is based on fracture mechanics and directly links the changes in material structure resulting from environmental deterioration processes to composite flexural mechanical properties. The model was used as a tool to estimate quantitatively cellulose fiber-matrix interfacial microparameters that were too difficult to measure experimentally. Reasonable agreement was found between model predictions and experimentally determined trends in composite flexural mechanical properties and mode of cellulose fiber failure (pullout or rupture) as a function of environment. This supports the validity of the proposed micromechanical modeling parameters. © 1999 Elsevier Science Ltd. All rights reserved.

Asbestos fibers were used extensively by the fiber cement industry as thin sheet cement composite reinforcement until studies showed exposure to asbestos caused lung cancer, asbestosis, and mesothelioma in humans [1]. Use of asbestos was discontinued, sparking extensive research into alternative fiber systems. Requirements placed upon the alternative fiber were high mechanical properties, high processability, and long-term durability in an alkali-rich cementitious environment. Cellulose fibers fulfilled the first two requirements. Cellulose fibers are intrinsically strong, and refinement (or mechanical beating) of the cellulose fibers greatly improves their processability, necessary if the composite is to be manufactured successfully using the Hatschek production method [2–4]. However, when cellulose fiber-reinforced cement composites were exposed to an outdoors environment, composite performance and mechanical properties changed, implying poor durability [5]. Microstructural study of the composite using scanning electron microscopy revealed that the cellulose fiber structure and the fibermatrix contact area were affected by changing environment [6–8].

This paper focuses on identifying changes in the material structure of dry refined and unrefined cellulose fiber composites after exposure to water and accelerated aged (carbonation) environments and linking these changes to composite mechanical properties via a micromechanics-based durability model. The composite material structure is subdivided into three areas: fiber, matrix, and fiber-matrix interfacial transition zone. Micromechanical parameters are used to describe the material structure: fiber parameters for strength, stiffness, length and diameter, matrix parameters for stiffness, fracture toughness, and initial flaw size and fiber-matrix interaction parameters for interfacial frictional and chemical bond and snubbing coefficient. A flexural micromechanics-based model uses these input parameters to predict composite mechanical properties [9]. Quantifying the effect of changing environment on the micromechanical parameters will allow the model to be used for composite durability prediction. This forward prediction is possible if the micromechanical parameters can be measured experimentally. However, the cellulose fiber-matrix interfacial parameters cannot be measured directly because the fiber is too small. The single fiber pullout technique cannot be used. Therefore, the model will serve as a tool to estimate the bond of the cellulose fiber to the cement matrix and the effect of environment on this bond.

The fracture mechanics-based micromechanical model used to predict composite mechanical properties will be described. Special emphasis is placed on theoretically developing the composite's fiber bridging stress vs. crack open-

* Corresponding author. Tel.: 734-764-3668; Fax: 734-764-4292; E-mail: pjak@engin.umich.edu.

ing (σ_b-δ) relation recognized as the fiber composite's constitutive law [9–11]. Then, the micromechanical modeling parameters will be defined and the effect of environment on fiber related parameters and on fiber-matrix interaction parameters will be determined. Verification of the cellulose fiber composite's micromechanical properties used for modeling is obtained:

1. If the modeled flexural mechanical properties have the same magnitude and follow the same trends as the experimentally obtained flexural mechanical properties in dry, wet, and aged environments, and
2. If the model correctly predicts the mode of cellulose fiber failure, pullout, or rupture.

1. Flexural modeling: durability of cellulose cement

Cellulose fiber-reinforced thin sheet cement composites fail by cracking when loaded in flexure. A realistic description of composite failure is provided by fracture mechanics using a force equilibrium and deformation compatibility analysis [9]. Under load, an edge crack forms on the tension side of the thin sheet (Fig. 1). The effect of fibers bridging across the crack plane will be described using the fiber bridging stress vs. crack opening (σ_b-δ) relationship. Durability of cellulose composites is assessed theoretically by recognizing the influence changing environment (dry, wet, or aged) has on fiber, matrix, and interfacial properties, or as a whole, the σ_b-δ relation. These changes influence the composite's flexural mechanical properties and their load-deflection behavior.

1.1. Theoretical concepts of micromechanical modeling

An imposed initial crack (a pre-existing crack-like flaw) propagates from the tensile side of the plate under uniform bending moment to the compression side of the plate (Fig. 1). This single crack analysis is described by the coupled governing Eqs. (1) and (2). Crack extension occurs when the stress intensity factor at the crack tip, K_{tip}, equals the fracture toughness of the cementitious matrix, K_m:

$$K_{tip} \equiv K_a + K_b = K_m \tag{1}$$

where K_{tip} is a function of external applied moment m, crack length a, plate geometry, and the fiber bridging stress vs. crack opening relation. It is the sum of K_a, stress intensity factor due to applied loading, and K_b, negative stress intensity factor due to fiber bridging stress (Appendix A).
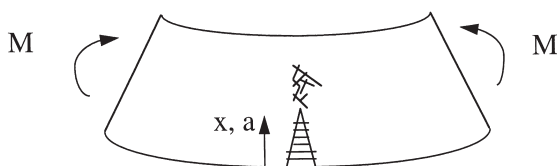

Fig. 1. Model schematic of thin sheet in bending.

Eq. (2) is based on Castigliano's theorem that relates equilibrium load (σ_M due to flexural loading) to the crack opening profile $\delta(x)$.

$$\frac{\delta(x)}{2} = \frac{4}{E}\int_x^a \left(\int_0^{a'} G(x',a',w)[\sigma_M(x') - \sigma_b(\delta(x'))]dx' \right)$$
$$G(x,a',w)da' \tag{2}$$

where G() is a weight function that represents a unit force contribution to crack tip stress intensity factor (Appendix A), $\delta(x)$ is the crack opening profile, $\sigma_M(x')$ is bending stress induced by external loading M, and $\sigma_b(\delta(x'))$ is bridging stress vs. crack opening relationship with x measured from the tensile side of the beam. E and w are composite elastic modulus and beam depth, respectively.

The coupled Eqs. (1) and (2) must be solved numerically [10]. For each imposed incremental crack length a, the equilibrium load M is calculated to yield composite mechanical properties. Limit of proportionality (LOP), or composite first crack strength, is the composite flexural stress carried when the initial flaw propagates. Modulus of rupture (MOR) is defined as the composite's maximum flexural stress.

For a composite with randomly distributed discontinuous fibers of volume fraction V_f, Li et al. [12] showed that the composite σ_b-δ relation in Eq. (3) can be predicted by averaging over the contributions of only those individual fibers crossing the crack plane:

$$\sigma_b(\delta) = \frac{4V_f}{\pi d_f^2} \int_{\theta=0}^{\frac{\pi}{2}} \int_{z=0}^{\frac{L_f}{2}\cos\theta} P(\delta)e^{f\theta}p(\theta)p(z)dzd\theta \tag{3}$$

where L_f, d_f, and f are fiber length, fiber diameter, and snubbing coefficient, respectively, and p(z) and p(θ) are centroidal and angular probability density functions. P(δ) is the single fiber load-displacement relation for aligned fibers.

For uniform two-dimensional fiber distribution, p(θ) = $2/\pi$ and p(z) = $2/L_f$. Effects of environmental deterioration processes enter through the mechanistic part of the σ_b-δ relation, P(δ) $e^{f\theta}$, calculated using fiber, matrix, and fiber-matrix interaction micromechanical parameters. The fiber bridging stress vs. crack opening (σ_b-δ) relationship is input to Eqs. (1) and (2).

Another (but consistent) model is used to predict composite flexural toughness from a three-point bending load-deflection simulation. Composite flexural toughness (IMOR) is the area under the load-deflection curve up to MOR. IMOR prediction is necessary for durability modeling because deterioration processes can significantly affect composite toughness [4,13]. When the bridging fibers are replaced by an equivalent bridging stress distribution at each equilibrium state of the plate or thin sheet, the composite can be treated as a linear elastic body. The only loads are the bending load and the fiber-induced applied traction to the face of the crack. The supports act as displacement constraints. The principle of superposition applies, so the load-point deflection Δ can be obtained as in Eq. (4) (Fig. 2):
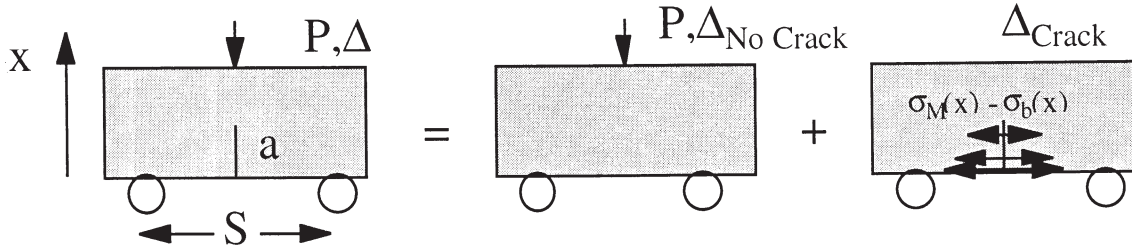
Fig. 2. Superposition scheme for load-point deflection calculation.

$$\Delta = \Delta_{no\ crack} + \Delta_{crack} \qquad (4)$$

where $\Delta_{no\ crack}$ is uncracked plate deflection and Δ_{crack} is cracked plate deflection (Appendix B). Load, crack length, and fiber bridging stress can be obtained at each equilibrium step from the micromechanical model. The load-deflection curve can then be generated.

1.2. Micromechanical modeling parameters

Using the micromechanics-based model, composite flexural performance is described by 11 micromechanical properties of the fiber-matrix system [9]. These fiber, matrix, and fiber-matrix interaction properties govern how the fibers bridge the crack. Therefore, they play a critical role in controlling the flexural response of the plate. Specimen geometry (thickness, span, and width) are also input parameters. The micromechanical modeling parameters are defined as follows:

Fiber parameters:
   L_f, fiber length (mm)
   d_f, fiber diameter (μm)
   E_f, fiber stiffness (GPa)
   σ_{fu}, fiber strength (MPa)
   V_f, fiber volume fraction (%).

Matrix parameters:
   E_m, matrix stiffness (GPa)
   K_m, matrix fracture toughness (MPa $\sqrt{m}$)
   c, initial flaw size (μm).

Fiber-matrix interaction parameters:
   τ_o, interfacial frictional bond (MPa)
   G_d, interfacial chemical debond energy (J/m^2)
   f, fiber snubbing coefficient.

Specimen geometry parameters:
   S, flexural specimen span (mm)
   b, flexural specimen thickness (mm)
   w, flexural specimen width (mm).

2. Experimental testing of cellulose cement

Cellulose fiber-reinforced thin sheet cement composites ($V_f = 10\%$) were produced in the laboratory using a filter-press technique (200 $\times$ 78 $\times$ 6 mm^3). Water-to-cement ratio was 0.25. Cellulose fibers had a two-dimensional ran-

dom orientation within the composite. Both refined (150 CSF) and unrefined (700 CSF) kraft pulped *Pinus radiata* cellulose fibers were used. Composites (28 days air cured) were tested in three-point bending with a span of 146 mm at 20 mm/min under dry and wet conditions. Wet conditions were defined as immersion of the composite in water 24 to 36 h before testing. In addition, accelerated aged specimens were tested air-dry to examine the aging effect of 30 carbonation cycles. Carbonation cycles have been shown to simulate accurately the effects of long-term natural weathering on cellulose composites [5]. One 24 h carbonation cycle is as follows:

   8 h submerged in water at 20°C
   1 h in the oven at 80°C
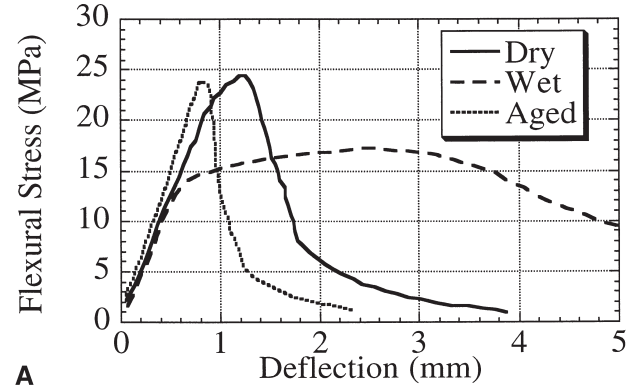
A
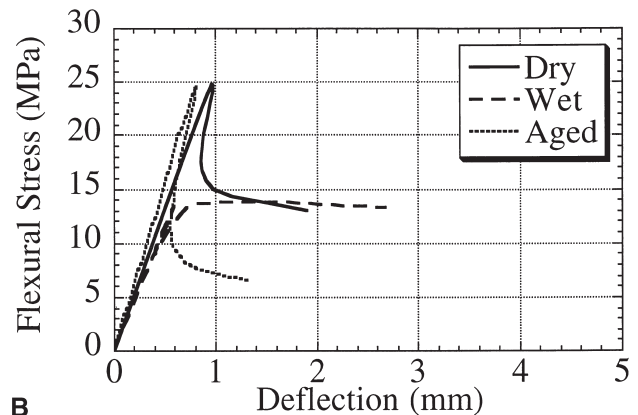
B

Fig. 3. (*A*) Experimentally tested refined cellulose composites. (*B*) Modeled refined cellulose composites.
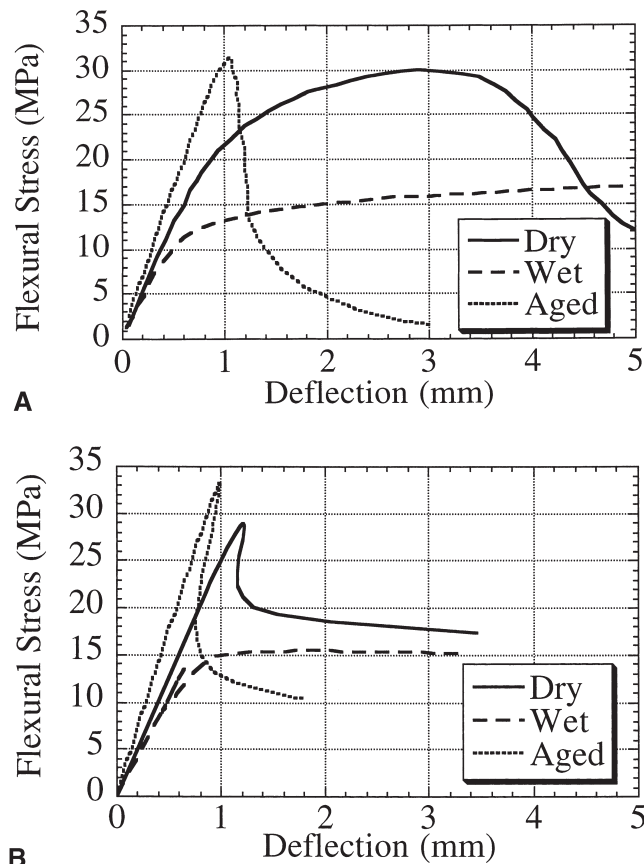
Fig. 4. (*A*) Experimentally tested unrefined cellulose composites. (*B*) Modeled unrefined cellulose composites.

5 h in the oven at 20°C in a saturated CO_2 environment

9 h in the oven at 80°C

1 h cooling down from 80°C to 20°C [5].

Experimental flexural load-deflection curves for the composites are shown in Figs. 3A and 4A for the refined and the unrefined cellulose composites, respectively. The model predictions (Figs. 3B and 4B) will be discussed in a later section. Environmental trends in composite mechanical properties can be summarized: $LOP_{aged} > LOP_{dry} > LOP_{wet}$, $MOR_{aged} \geq MOR_{dry} > MOR_{wet}$, and $IMOR_{aged} < IMOR_{dry} < IMOR_{wet}$. Likewise, mode of cellulose fiber failure changed with environmental conditions: dominant rupture for aged, combination of pullout/rupture for dry, and pullout for wet. The dry and wet composites failed by multiple cracking, whereas the aged composites failed with one crack. These trends hold regardless of whether the cellulose fibers were refined or unrefined.

3. Determination of micromechanical modeling parameters

Cellulose fiber and matrix microparameters were extracted from literature, but the cellulose fiber-matrix interfacial pa-

rameters are not available. They have not been determined experimentally due to the unavailability of long *Pinus radiata* cellulose fibers for single fiber pullout testing. Therefore, the model can serve as a valuable tool for their estimation. The estimated interfacial modeling parameters (τ_o, G_d, and f) are influential in predicting the environmentally dependent composite flexural mechanical properties (LOP, MOR, and IMOR). Likewise, they determine the mode of cellulose fiber failure, rupture, or pullout.

3.1. Cellulose fiber parameters

Cellulose is a hollow natural organic hydrophilic wood fiber composed of fibrils concentrically layered around a composite tube. When loaded in tension, the cellulose fiber's cross-sectional area reduces [14]. Fiber properties, structure, and mechanical reinforcing ability are highly variable, depending on wood fiber source and method of pulping [15]. Micromechanical modeling parameters were chosen to represent the average property value of dry refined kraft pulped *Pinus radiata* cellulose fibers (Table 1). They are based on measured values (L_f and d_f) and literature review (σ_{fu} and E_f) [4,16]. Highly refined cellulose fibers (150 CSF) have lengths varying from 0.1 to 7 mm with a mean of 2.5 mm. Likewise, fiber diameter varies significantly with an average value of 30 μm. Tensile testing of the cellulose fiber in a wet environment shows a loss of fiber stiffness, whereas fiber strength does not change when compared to dry, but the fibers do experience greater extension [16]. After aging, cellulose fibers petrify and fail in a brittle manner; fiber stiffness and strength have been speculated to increase [6]. For modeling simplicity, fiber strength was kept constant regardless of environment. Unrefined cellulose fibers (700 CSF) have improved mechanical properties (Table 1). Refinement causes fiber length to decrease, fiber strength to decrease because of external fibrillation, and fiber stiffness to decrease because of internal fibrillation that makes the fiber more conformable [2].

3.2. Cellulose fiber-matrix interaction parameters

The cellulose fiber-matrix interfacial bond, reflected in the changed mode of cellulose fiber failure at the composite

Table 1
Refined and unrefined cellulose micromechanical modeling parameters for dry, wet, and aged environments

	Refined			Unrefined		
	Dry	Wet	Aged	Dry	Wet	Aged
L_f (mm)	2.5	2.5	2.5	4	4	4
d_f (μm)	30	30	30	30	30	30
E_f (GPa)	30	**10**	40	35	**12**	47
σ_{fu} (MPa)	550	550	550	650	650	650
τ_o (MPa)	**0.8**	**0.8**	**3.0**	**0.6**	**0.6**	**2.3**
G_d (J/m^2)	**3.0**	**1.0**	**3.5**	**3.0**	**1.0**	**3.5**
f	**0.8**	**0.5**	**0.8**	**0.7**	**0.4**	**0.7**
E_m (GPa)	15.4	13.5	18.0	14.9	12.2	20.3

Boldface indicates estimated values.

fracture surface, varies with environment (dry, wet, and aged). The bond of the cellulose fiber to the cement matrix is frictional and chemical in nature, quantified by frictional bond (τ_o) and chemical debonding energy (G_d) [3,9]. An approximation of the dry refined cellulose fiber's frictional bond ($\tau_o = 0.8$ MPa) was made by Mai [17] using theoretical composite modeling. A moderate value of ($G_d = 3$ J/m^2) was assumed. Chemical debond energy is defined as the critical interfacial debonding energy required to advance unit area of the debonding zone. Dry cellulose fibers lock into the rigid cement matrix by a large number of hydrogen bonds via hydroxyl bridging sites [3]. For comparison, typical toughness of cement pastes varies from 2 to 10 J/m^2. The snubbing coefficient, which represents the effect of a fiber pulled at an angle over a friction pulley, has not been determined for cellulose fibers. It was found to vary from 0.7 to 0.9 for polypropylene and nylon fibers, respectively [18]. The varible f was assumed to be 0.8 for dry refined cellulose fibers. Even though polypropylene and cellulose fibers are not chemically similar, it is assumed that, mechanically, their snubbing coefficient will be comparable and of the same order of magnitude.

The cellulose fiber's frictional bond was assumed to remain constant regardless of dry or wet conditions. The basis for this assumption is experimental. Single fiber pullout test data obtained using polypropylene and PVA fibers showed negligible changes in their τ_o values for dry and wet conditions [19]. The effect of environment on the interfacial bond properties of polypropylene and PVA fibers is used as guidance for similar bond property changes between the cellulose fiber and cement matrix. Under wet conditions, it is speculated that insertion of water molecules between the cellulose fibers and the matrix breaks their fibermatrix hydrogen bonds [3]. Loss of chemical bond would support observed cellulose fiber pullout under wet conditions compared with combination pullout and rupture under dry conditions. G_d of 1 J/m^2 was chosen. Snubbing coefficient of the wet cellulose fibers was lowered to 0.5 because fiber stiffness drops when wet.

After accelerated aging, cellulose fibers petrify and have a solid cross-section. PVA, a solid fiber having a different chemical composition from that of the cellulose fiber, bonds frictionally and chemically with cement. The PVA-cement frictional bond increased significantly (~300%) after carbonation aging [19], so 3.0 MPa was deemed suitable for cellulose fibers. Aging causes the interfacial matrix to densify and to increase contact with the reinforcing fibers [8]. The PVA chemical bond increased slightly after accelerated aging. This was reflected in the choice of the aged cellulose fiber's chemical bond, 3.5 J/m^2. The dry snubbing coefficient of 0.8 was retained for aged conditions.

For unrefined cellulose fibers, interfacial frictional bond and snubbing coefficient were lowered compared to refined to account for less cellulose fiber fibrillation [20]; τ_o decreased to 0.6 MPa and f decreased to 0.7. The chemical bond remained the same. It was assumed that changing environment would cause the same percent changes in interfacial

properties for unrefined as for refined cellulose fibers. The values chosen in modeling for the floating parameters of τ_o, G_d, and f are not tuned to match the cellulose fiber composite experimental data precisely. Instead, these values are intended to predict the trend in flexural mechanical properties of cellulose cement with changing environment. The actual values of these parameters for refined and unrefined cellulose fibers may differ from these estimated values.

Fracture toughness of a cementitious matrix having a similar water-to-cement ratio as that of the experimentally tested composites was used; $K_m = 0.2$ MPa $\sqrt{m}$ [21]. The initial unbridged flaw size, c, was chosen to be 60 μm based on scanning electron microscopic examination of thin sheet composites. K_m and c were assumed constant, unaffected by changing environment. These simplifying matrix assumptions were made to aid in identifying the effects of changing environment on cellulose fibers and cellulose fiber-matrix interfacial properties only. Fiber volume fraction (V_f), specimen size (S × w × b) and composite stiffness (E_m) used in modeling were chosen to match experimental values.

Using these micromechanical modeling parameters, the σ_b-δ relation for the refined and the unrefined cellulose fiber composites under dry, wet, and aged conditions can be generated (Figs. 5A and 5B). The high bridging stress at very small crack opening (<0.002 mm) for dry and aged conditions in-
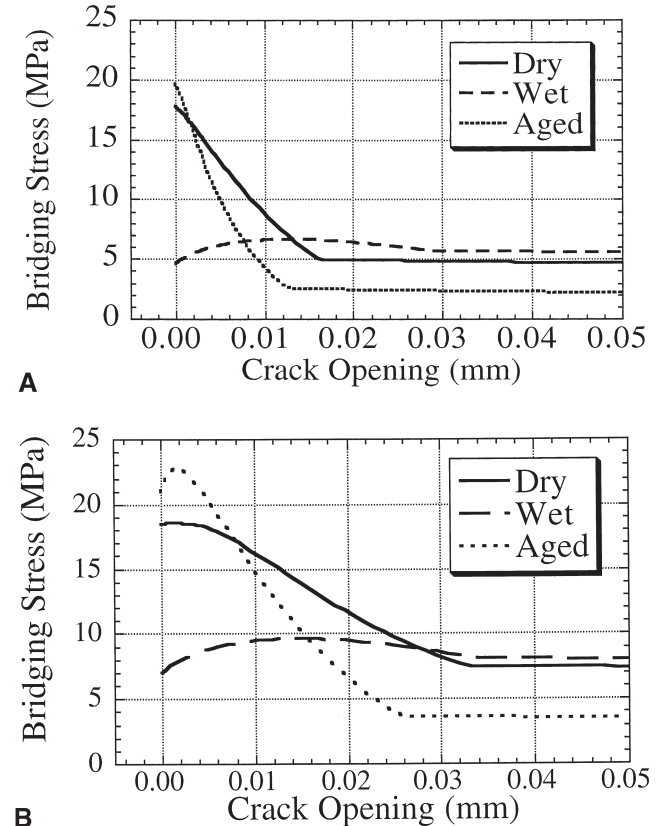

A

B

Fig. 5. (*A*) σ_b-δ Relation for refined cellulose. (*B*) σ_b-δ Relation for unrefined cellulose.

dicates high LOP compared with the low bridging stress of the wet composite (as seen in Figs. 3 and 4). The sharp decrease in bridging stress for the aged composites at large crack opening (0.03 mm) implies extreme fiber rupture. The slope of this transition (from small to large crack opening) decreases from aged to dry to wet. Similar trends are found for the unrefined cellulose fiber composites (Fig. 5B). Higher bridging stress for unrefined cellulose fibers can be attributed to improved fiber properties (Table 1).

4. Model verification

Comparison of experimental and modeled flexural stress-deflection curves for refined and unrefined cellulose fiber composites is provided in Figs. 3A, 3B, 4A, and 4B. The model correctly predicts the trends in composite properties (LOP and MOR) with changing environment, yet there is a discrepancy when predicting composite toughness (IMOR) for dry and wet conditions (Fig. 6). This is attributed to the one crack to failure assumption of the model. If the modeled toughness were multiplied by the number of multiple cracks formed under dry and wet conditions, model predictions would be more accurate. However, the one crack to failure model does show the trend of increasing composite toughness with the transition from aged to dry to wet. The improved fiber properties of unrefined cellulose contributed to increased composite toughness. These reasonably good toughness agreements impart further confidence to model predictions.

To demonstrate fiber failure on the composite fracture surface through modeling for the refined and the unrefined cellulose fibers, an infinitely high fiber strength was assumed (Figs. 7A and 7B). This is compared with the case where fiber ruptures when a unique, deterministic fiber strength is reached. If fiber strength were infinitely high, the fiber would not rupture but would pullout. For the dry refined cellulose composite, these comparisons suggest that there is a combination of pullout and rupture while there is only pullout of the wet cellulose fibers (Fig. 7A). Under
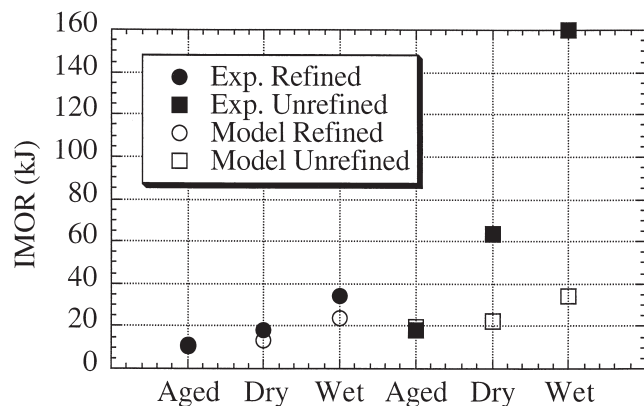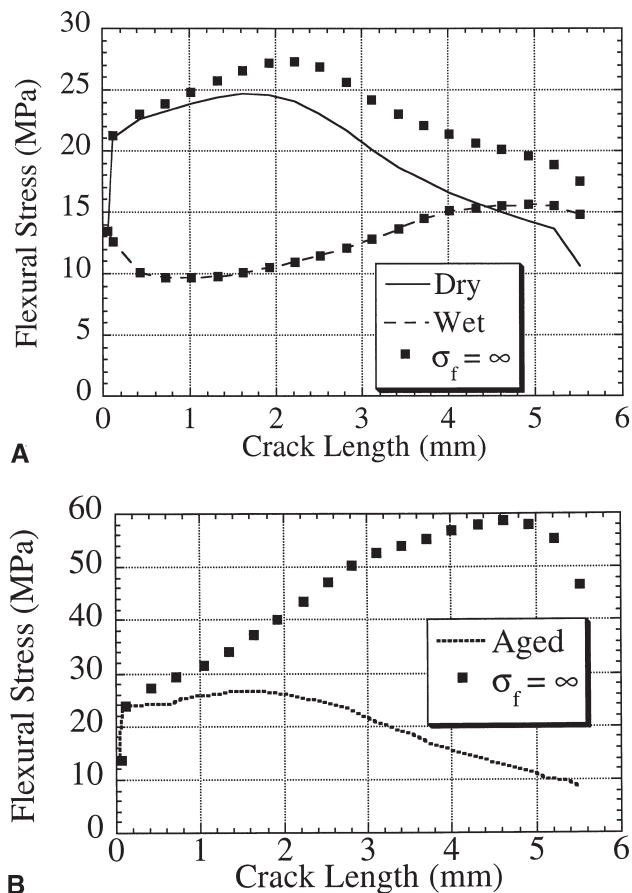

Fig. 7. (A) Demonstration of modeled dry and wet cellulose fiber failure. (B) Demonstration of modeled aged refined cellulose fiber failure.

aged conditions, this comparison indicates extreme fiber rupture (Fig. 7B). These trends are in accordance with experimental observations.

5. Conclusions

The following conclusions can be drawn from the current study:

1. The micromechanics-based model is capable of predicting broad trends in refined and unrefined cellulose cement's flexural strength and toughness (LOP, MOR, and IMOR) as a function of dry, wet, and accelerated (carbonation) aged environmental conditions.
2. For modeling purposes, changes in cellulose fiber properties and cellulose fiber-matrix interaction parameters with environment were estimated as follows for prediction of refined and unrefined cellulose cement's flexural composite performance:
   Fiber stiffness: $E_{f\,aged} > E_{f\,dry} > E_{f\,wet}$
   Fiber strength: $\sigma_{fu\,aged} \sim \sigma_{fu\,dry} \sim \sigma_{fu\,wet}$
   Interfacial frictional bond: $\tau_{o\,aged} > \tau_{o\,dry} \sim \tau_{o\,wet}$
   Interfacial chemical bond: $G_{d\,aged} > G_{d\,dry} > G_{d\,wet}$
   Snubbing coefficient: $f_{aged} \sim f_{dry} > f_{wet}$.

Fig. 6. Comparison of toughness trends for experimental and modeled refined and unrefined dry, wet, and aged composites.

3. Loss of cellulose cement toughness with aging is attributed to increased interfacial bonding of the cellulose fiber to the cement matrix, which causes increased fiber rupture.
4. Because experimental measurements of the interfacial properties of cellulose fibers to the cement matrix as a function of environment are not available, they must be back calculated from experimental composite flexural mechanical data using durability models. This inversion process is not expected to produce a unique set of interface parametric values. However, the durability models are capable of predicting performance of the cellulose composites as a function of environment and identifying the cellulose fiber-matrix interface as the component of the composite's material structure most affected by changing environment.

Acknowledgments

Appendix A

Crack tip stress intensity factor is attributed to applied stress and to fiber bridging stress. It is described as $K_{tip} = K_a + K_b$, where K_a = stress intensity factor due to applied loading and K_b = stress intensity factor due to fiber bridging stress. Furthermore, as given in Eq. (5):

$$K_a = 2\int_0^a G(x,a,w)\sigma_a(x)dx \qquad (5)$$

where a = crack length, w = plate depth,

$$\sigma_a(x) = \sigma_0\left(\frac{w}{2} - x\right)$$

σ_a = applied external stress at the tensile face, and x is measured from the tension face of the beam [23]. σ_o is related to the external bending moment through

$$\sigma_0 = \frac{6M}{bw^2}$$

where M = applied external bending moment and b = beam width.

G is a weight function that represents a unit force contribution to crack tip stress intensity factor, as follows:

$$G(x,a,w) = \frac{1}{\sqrt{\pi a}}\frac{h_1(x/a,a/w)}{(1-x^2/a^2)^{1/2}}$$

with h_1 given in [23]. Similarly,

$$K_b = -2\int_0^a G(x,a,w)\sigma_b(\delta(x))dx$$

where $\sigma_b(\delta)$ = fiber bridging stress vs. crack opening relation and $\delta(x)$ = crack opening profile. Because the crack opening profile is not known a priori, this requires solution of the integral Eq. (2).

Appendix B

$\Delta_{no\ crack}$ can be found by classic beam theory

$$\left(= \frac{PS^3}{4Eb^3w}\right)$$

where E = composite modulus and Δ_{crack} can be obtained by integration of Eq. (6):

$$\Delta_{crack} = w\int_0^a (\sigma_m(x) - \sigma_b(x))f(x)dx \qquad (6)$$

where w = plate width, a = crack length, $\sigma_m(x)$ = applied loading stress, $\sigma_b(x)$ = fiber bridging stress, x is measured from tensile side of plate and $f(x)$ = weight function corresponding to load-point displacement produced by a pair of unit concentrated forces at arbitrary location x along the crack line. $f(x)$ can be derived from Eq. (7) [22,23]:

$$f(x) = \frac{6\sqrt{2Sa}}{Eb^2w}F\left(\frac{a}{b}\right)\left[\left(1-\frac{x}{a}\right)\left(1+\frac{\lambda}{2}\left(1-\frac{x}{a}\right)\right)\right]^{1/2}$$

where

$$F\left(\frac{a}{b}\right) = \left(\frac{a/b}{1-a/b}\right)^2[5.58 - 19.57\left(\frac{a}{b}\right) + 36.82\left(\frac{a}{b}\right)^2$$
$$-34.94\left(\frac{a}{b}\right)^3 + 12.77\left(\frac{a}{b}\right)^4,$$

$$\lambda = \frac{V_1^2}{F^2} - 2$$

and

$$V_1\left(\frac{a}{b}\right) = 0.76 - 2.28\left(\frac{a}{b}\right) + 3.78\left(\frac{a}{b}\right)^2 - 2.04\left(\frac{a}{b}\right)^3 \qquad (7)$$
$$+ \frac{0.66}{(1-a/b)^2}$$

References

[1] J.B. Studinka, Int J Cem Comp Ltwt Concr 2 (1989) 73–78.
[2] R.S.P. Coutts, Composites 15 (2) (1984) 139–143.
[3] R.S.P. Coutts, P. Kightly, J Mater Sci 19 (1984) 3355–3359.
[4] A. Bentur, S. Mindess. Fiber Reinforced Cementitious Composites, Elsevier Applied Science, New York 1990.
[5] S.A.S. Akers, J.B. Studinka, Int J Cem Comp Ltwt Concr 11 (2) (1989) 93–97.
[6] A. Bentur, S.A.S. Akers, Int J Cem Comp Ltwt Concr 11 (2) (1989) 99–109.

[7] R.S.P. Coutts, P. Kightly, J Mater Sci 17 (1982) 1801–1806.

[8] B.J. Pirie, F.P. Glasser, C. Schmitt-Henco, S.A.S. Akers, Cem Concr Comp 12 (1990) 233–244.

[9] Z. Lin, T. Kanda, V.C. Li, On interface property characterization and performance of fiber reinforced cementitious composites, submitted to J Conc Sci & Engineering.

[10] B.N. Cox, D.B. Marshall, Acta Metall Mater 39 (4) (1991) 579–589.

[11] V.C. Li, Z. Lin, T. Matsumoto, Influence of fiber bridging on structural size-effect, Int J Solids Struct 35 (31–32) (1998) 4223–4238.

[12] V.C. Li, Y. Wang, S. Backer, J Mech Phys. Solids 39 (5) (1991) 607–625.

[13] P. Soroushian, J.H. Won, Proc Int Symp Brittle Matrix Compos 4 (1994) 381–390.

[14] D.H. Page, F. el-Hosseiny, K. Winkler, Nature 229 (1971) 252–253.

[15] M.D. Campbell, R.S.P. Coutts, J Mater Sci 15 (1980) 162–170.

[16] Y.W. Mai, M.I. Hakeem, J Mater Sci 19 (1984) 501–508.

[17] Y.W. Mai, Applications of Fracture Mechanics to Reinforced Concrete, Elsevier Applied Science, New York, 1990, pp. 201–231.

[18] Y. Wang, Mechanics of fiber reinforced concrete, Doctoral thesis, MIT, Cambridge, MA, 1989.

[19] P.J. Kim, Unpublished data.

[20] X. Lin, M.R. Silsbee, D.M. Roy, Mater Res Soc Symp Proc 370 (1995) 487–496.

[21] V.C. Li, D.K. Mishra, H.C. Wu, Mater Struct 28 (1995) 586–595.

[22] H. Tada, The Stress Analysis of Cracks Handbook, second edition. Paris Proc. Inc., St. Louis, MO, 1985.

[23] X. Wu, Weight Functions and Stress Intensity Factor Solutions, 1st edition. Pergamon Press, New York, 1991.